iScience, Volume *23*

Supplemental Information

Membrane Estrogen Receptor (GPER) and Follicle-Stimulating Hormone Receptor (FSHR) Heteromeric Complexes Promote Human Ovarian Follicle Survival

Livio Casarini, Clara Lazzaretti, Elia Paradiso, Silvia Limoncella, Laura Riccetti, Samantha Sperduti, Beatrice Melli, Serena Marcozzi, Claudia Anzivino, Niamh S. Sayers, Jakub Czapinski, Giulia Brigante, Francesco Potì, Antonio La Marca, Francesco De Pascali, Eric Reiter, Angela Falbo, Jessica Daolio, Maria Teresa Villani, Monica Lispi, Giovanna Orlando, Francesca G. Klinger, Francesca Fanelli, Adolfo Rivero-Müller, Aylin C. Hanyaloglu, and Manuela Simoni

List of supplementary materials

Supplementary Images

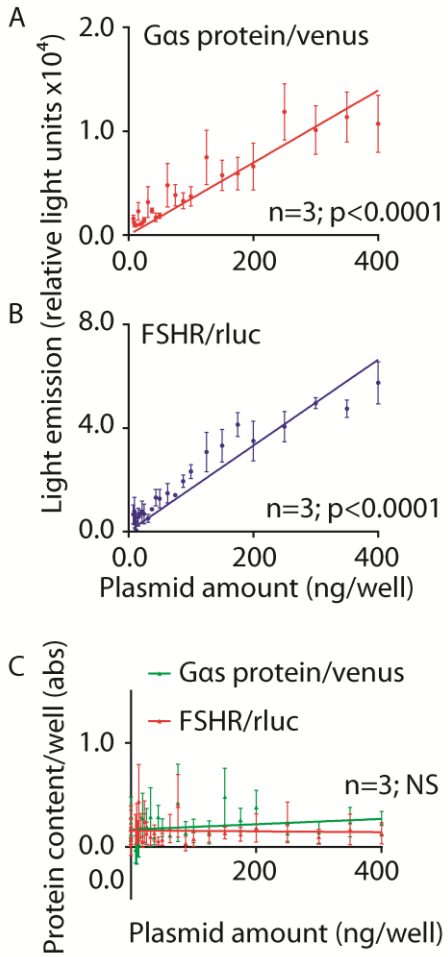

Figure S1. Control of cell transfection efficiency using FSHR and Gαs BRET biosensors. (**A**, **B**) Linear correlation between amount of Gαs protein/venus- or FSHR/rluc-encoding plasmid administered per well, and amount of protein by transiently transfected HEK293 cells. Light emitted by the biosensors was measured by BRET and coelenterazine H was added as a substrate in samples expressing the FSHR/rluc-encoding plasmid 5 min before signal acquisition. Data (means ± SEM; n=3) were interpolated by linear regression forced to pass through x=0.0 and y=0.0. (**C**) Bradford's assay of HEK293 cells transfected with increasing concentrations of Gαs protein/venus- or FSHR/rluc-encoding plasmid (BRET loading control). Protein content was determined by 595 nm absorbance (means ± SEM; n=3) and data interpolated by linear regression. Related to Figure 1A.

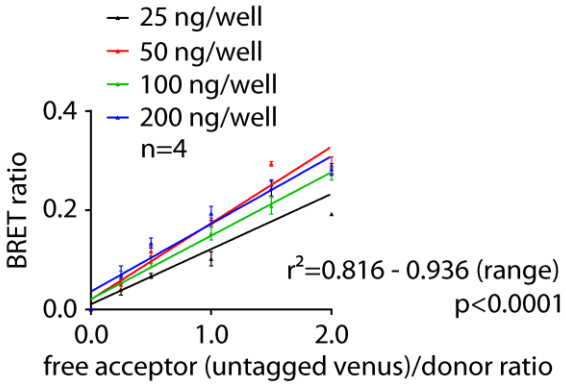

Figure S2. Negative control of FSHR/rluc and venus BRET signal specificity. HEK293 cells were transfected with the indicated concentrations of FSHR/rluc- and with increasing amount of untagged venus-encoding plasmid, then BRET signals were acquired by a plate reader and plotted as means ± SEM against acceptor/donor ratio (n=4). Data were interpolated by linear regression demonstrating the unspecific interaction between FSHR/rluc and untagged venus molecules. Related to Figure 1B-E.

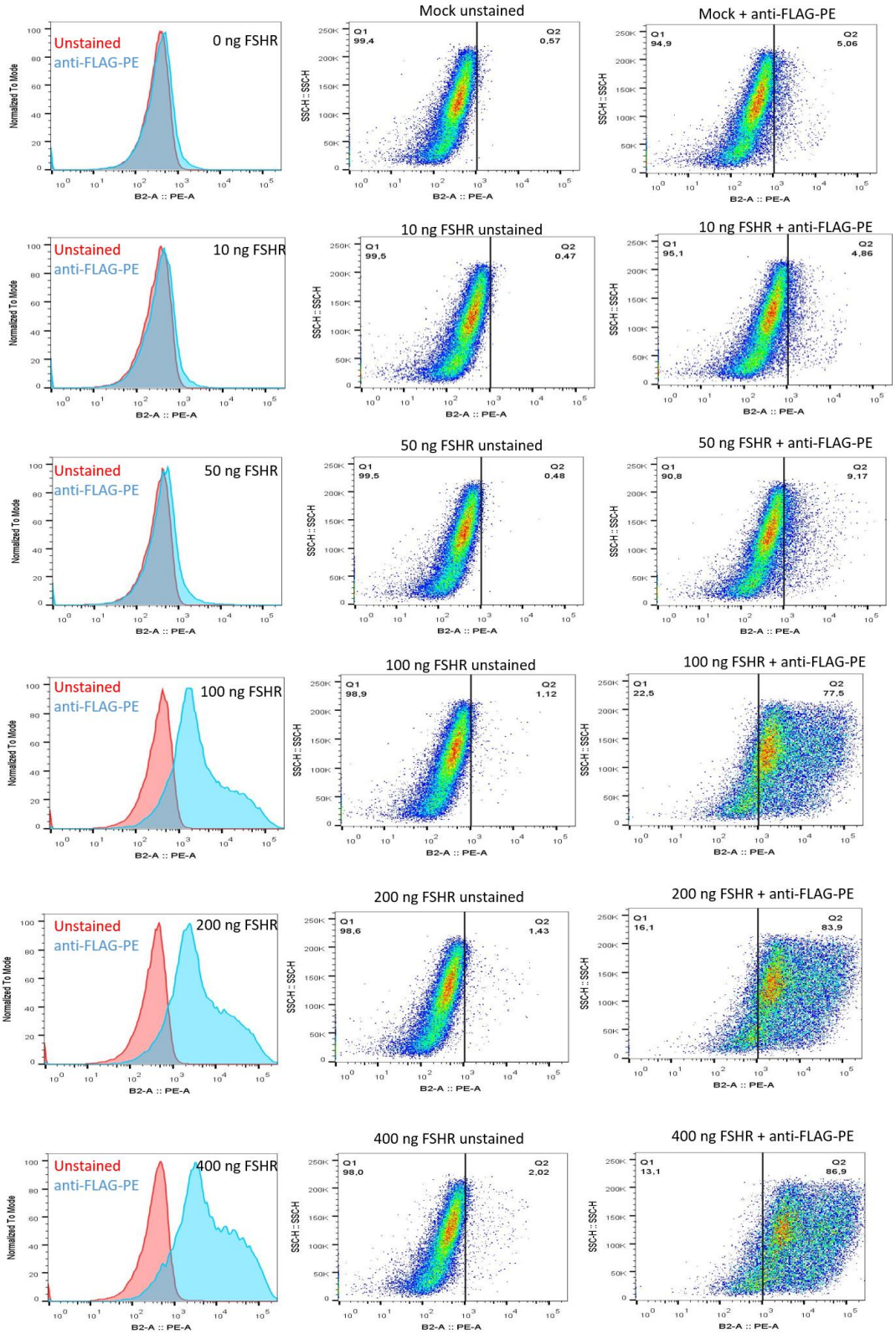
Unstained
anti-FLAG-PE
0 ng FSHR
Mock unstained
Mock + anti-FLAG-PE
10 ng FSHR
10 ng FSHR unstained
10 ng FSHR + anti-FLAG-PE
50 ng FSHR
50 ng FSHR unstained
50 ng FSHR + anti-FLAG-PE
100 ng FSHR
100 ng FSHR unstained
100 ng FSHR + anti-FLAG-PE
200 ng FSHR
200 ng FSHR unstained
200 ng FSHR + anti-FLAG-PE
400 ng FSHR
400 ng FSHR unstained
400 ng FSHR + anti-FLAG-PE
Normalized To Mode
SSC-H :: SSC-H
B2-A :: PE-A
Q1 99,4
Q2 0,57
Q1 94,9
Q2 5,06
Q1 99,5
Q2 0,47
Q1 95,1
Q2 4,86
Q1 99,5
Q2 0,48
Q1 90,8
Q2 9,17
Q1 98,9
Q2 1,12
Q1 22,5
Q2 77,5
Q1 98,6
Q2 1,43
Q1 16,1
Q2 83,9
Q1 98,0
Q2 2,02
Q1 13,1
Q2 86,9

Figure S3. Flow cytometry analysis of plasma membrane FSHR expression levels at different concentrations. 5 x 10^5 HEK293 cells were transfected either with mock vector or increasing concentrations of FLAG-FSHR-encoding plasmid (10-400 ng/well). Then, cells were stained with anti-FLAG-PE antibody for detection of FSHR and analyzed by flow cytometry. Red peaks in histograms refer to unstained cells while light blue peaks refer to cells incubated with anti-FLAG-PE. Total number of cells in each peak was normalized to 100 % (normalized to mode). Dot-plots show side-scatter versus PE-intensity. Q1 represents the percentage of unstained cells and Q2 the percentage of stained cells for each dot-plot. Related to Figure 1B-E.

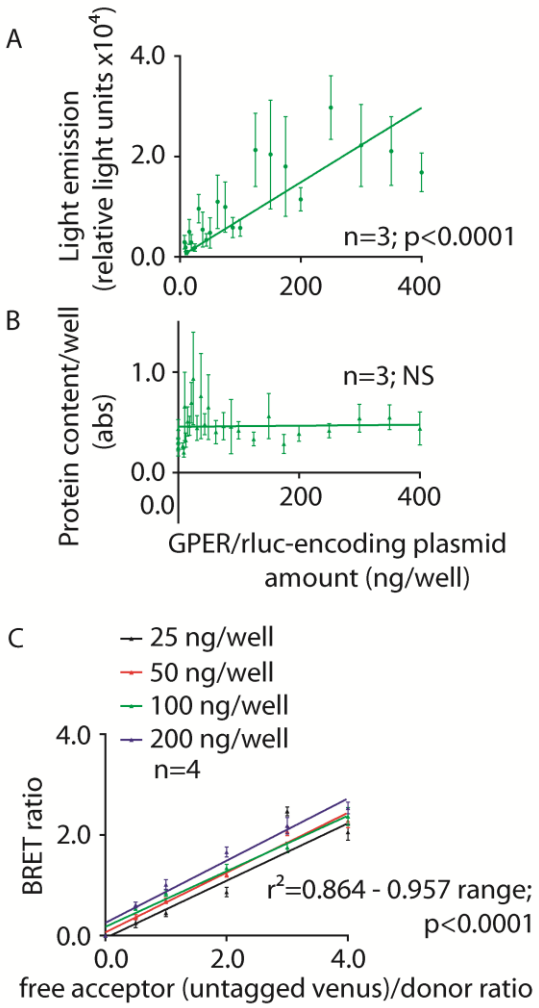

Figure S4. Control of cell transfection efficiency and signal specificity using the GPER BRET biosensors. (**A**) Linear correlation between amount of GPER/rluc-encoding plasmid per well and protein encoded, in transfected HEK293 cells. Light emitted by the biosensors was measured by BRET 5 min after addition of coelenterazine H. Data were interpolated by linear regression forced to pass through x=0.0 and y=0.0 (means ± SEM; n=3). (**B**) BRET loading control determined by Bradford's assay. HEK293 cells were transfected with increasing concentrations of GPER/rluc-encoding plasmid and the protein content was detected (absorbance at 595 nm), plotted as means ± SEM against the amount of plasmid per well and interpolated by linear regression (n=3). (**C**) Negative control of GPER/rluc and venus BRET signal specificity. HEK293 cells were transfected with the indicated concentrations of GPER/rluc- and with increasing amount of untagged venus-encoding plasmid, then BRET signals were acquired and plotted against the

acceptor/donor ratio (means ± SEM; n=4). Data interpolation by linear regression demonstrates the unspecific interaction between GPER/rluc and untagged venus molecules. Related to Figure 2F.

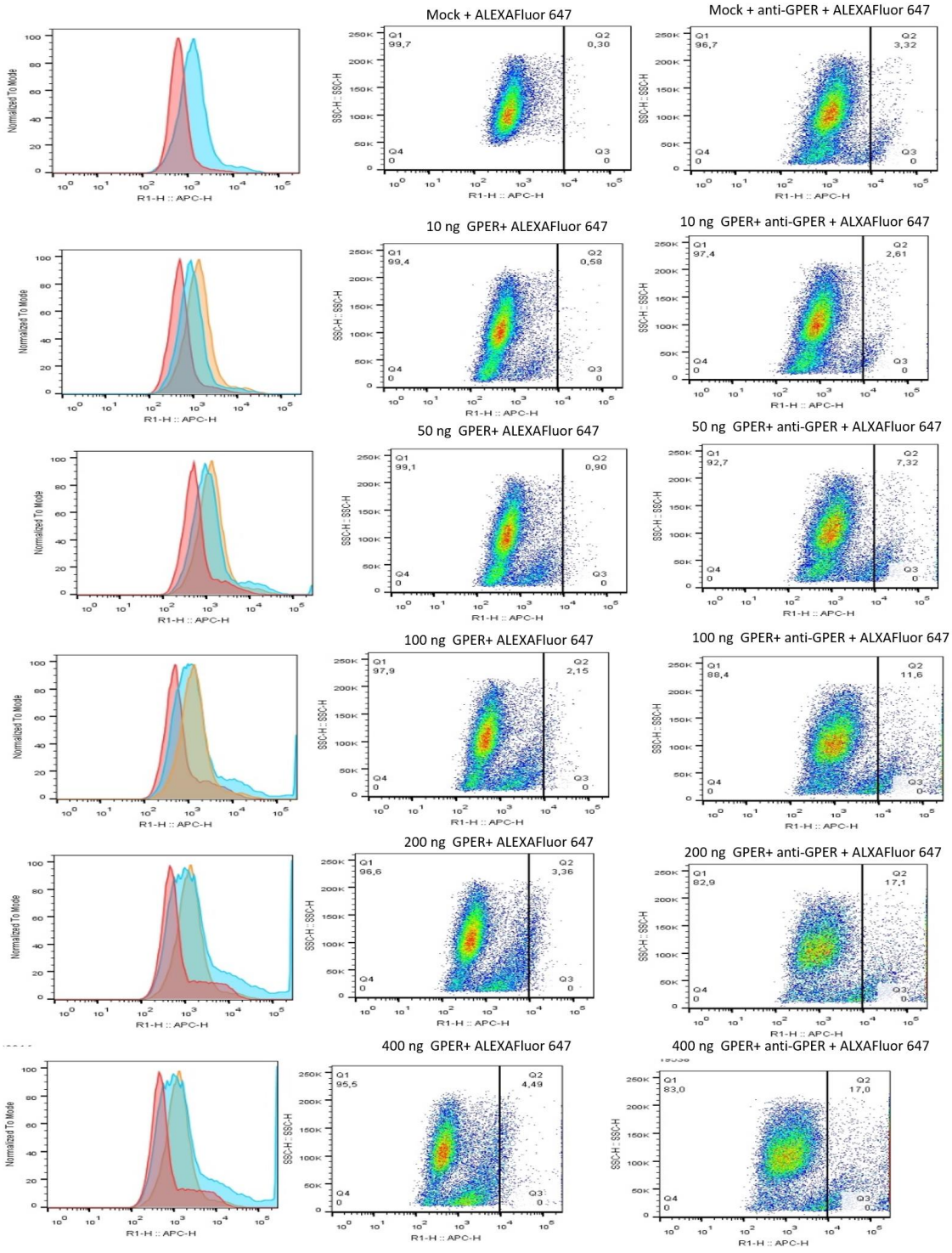

Figure S5. Flow cytometry analysis of plasma membrane GPER expression levels at different concentrations. 5 x 10^5 HEK293 cells were transfected either with mock vector or increasing concentrations of GPER-encoding plasmid (10-400 ng). Then, cells were

incubated with anti-GPER primary antibody followed by incubation with ALEXA Fluor 647 secondary antibody and analyzed by flow cytometry. Red peaks in histograms refer to cells incubated with secondary antibody only, light blue peaks refer to cells incubated with primary and secondary antibody while orange peaks refer to mock-transfected cells incubated with primary and secondary antibodies. Total number of cells in each peak was normalized to 100 % (normalized to mode). Dot-plots show side-scatter versus ALEXA Fluor 647 (APC-H) intensity. Q1 represents the percentage of cells negative to ALEXA FLUOR 647 staining and Q2 the percentage of cells positive to ALEXA FLUOR 647 staining in each dot-plot. Related to Figure 2F.

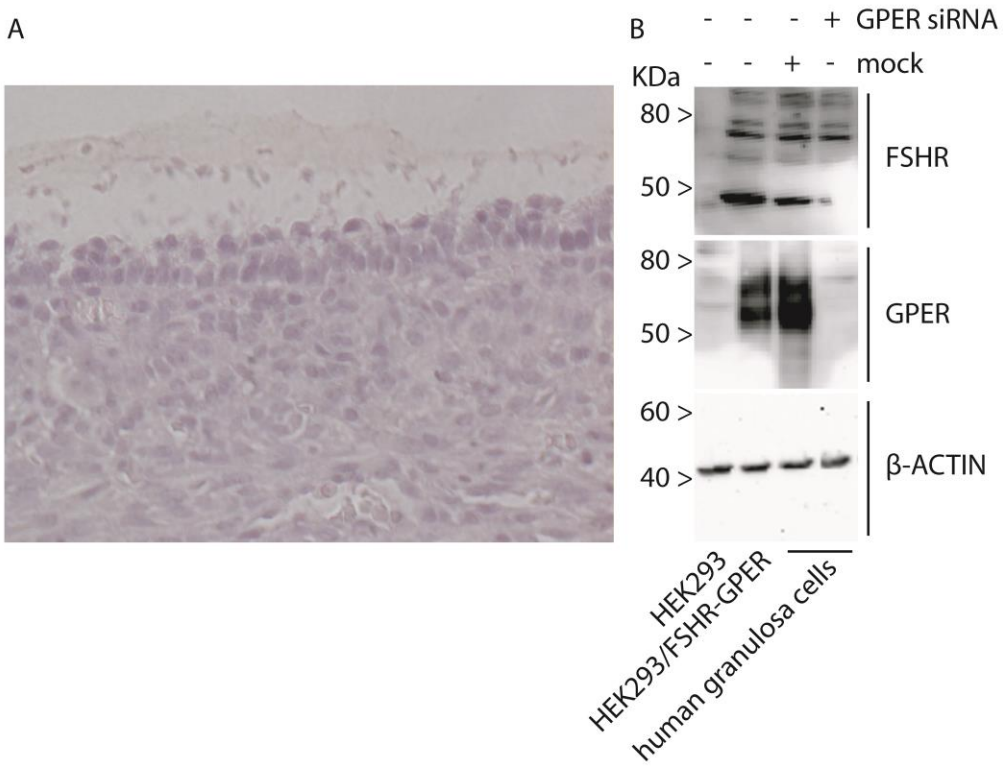

Figure S6. Antibody validations (**A**) Control section of IHC for FSHR and GPER. The same area was analyzed in serial sections, respectively incubated with anti-FSHR or anti-GPER antibodies or in absence of primary antibody (control). No staining was observed in this area indicating the specific signal of FSHR and GPER. (**B**) Uncropped Western blotting pictures using anti-FSHR, -GPER and -β-ACTIN antibodies (Fig. 1C). Membrane incubation with anti-FSHR antibody results in a number of known bands, as previously described (Casarini et al., 2016). The anti-GPER antibody may produce 52-58 KDa bands, as described by studies (Cheng et al., 2014) and providers (see: https://www.genetex.com/Product/Detail/GPR30-antibody-C2C3-C-term/GTX107748, last accession on April, 25th 2020). Related to Figure 6A, B, D.

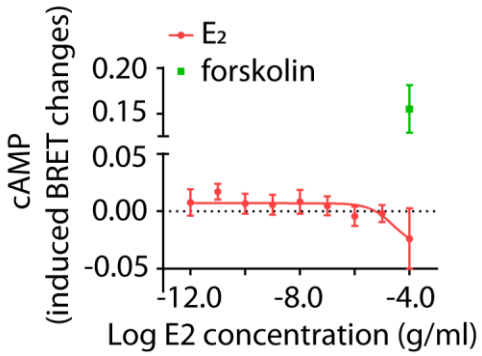

Figure S7. Failure of E_2-induced cAMP increase via GPER. Transfected HEK293 cells expressing GPER and the cAMP biosensor CAMYEL were treated 30 min with increasing E_2 concentrations (1.0 pg/ml-100 µg/ml range), in the presence of the phosphodiesterase inhibitor IBMX, before cAMP measurement by BRET. Results were represented in the x-y graph as means ± SEM (n=5) and interpolated by non-linear regression. No significantly different cAMP levels *versus* the vehicle were found, except for the forskolin-treated cells serving as positive controls (two-way ANOVA with Sidak's correction for multiple tests; $p<0.000$). Related to Figure 3C.

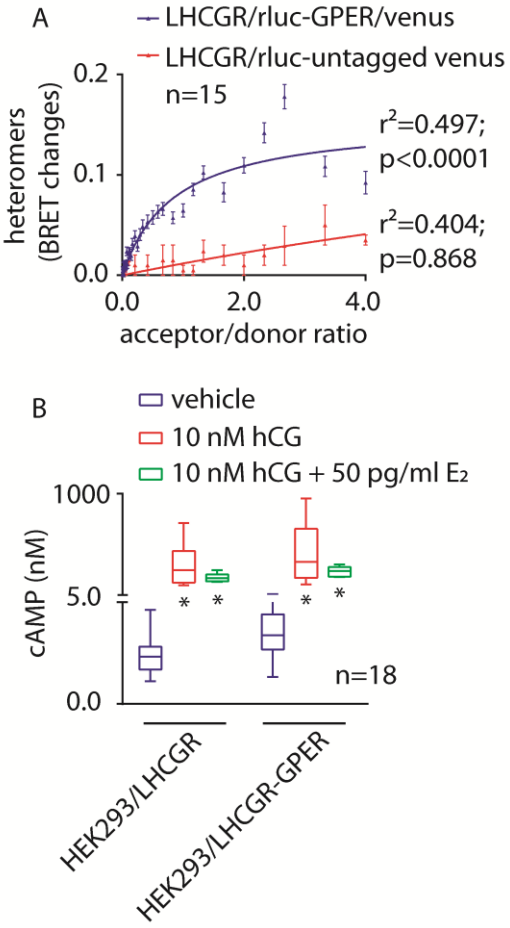

Figure S8. hCG-induced cAMP increase in the presence of LHCGR and GPER heteromers. (**A**) BRET signal demonstrating the formation of LHCGR/rluc- and GPER/venus-tagged heteromers, in transfected HEK293 cells. BRET ratio values resulting from molecular interactions were represented in the x-y graph as means ± SEM (n=5). Specific binding is indicated by data interpolation using non-linear regression, which results in the logarithmic curve, while unspecific binding between LHCGR/rluc and untagged venus molecules is indicated by linear regression. (**B**) 10 nM hCG-induced intracellular cAMP increase, in HEK293 cells expressing either one or both LHCGR and GPER. 50 pg/ml E_2 was added as indicated. cAMP was measured by ELISA and represented by box and whiskers plots (*=significantly different *versus* vehicle-treated HEK293/LHCGR; two-way ANOVA with Sidak's correction for multiple tests; $p<0.0001$; n=18). Related to Figure 3F.

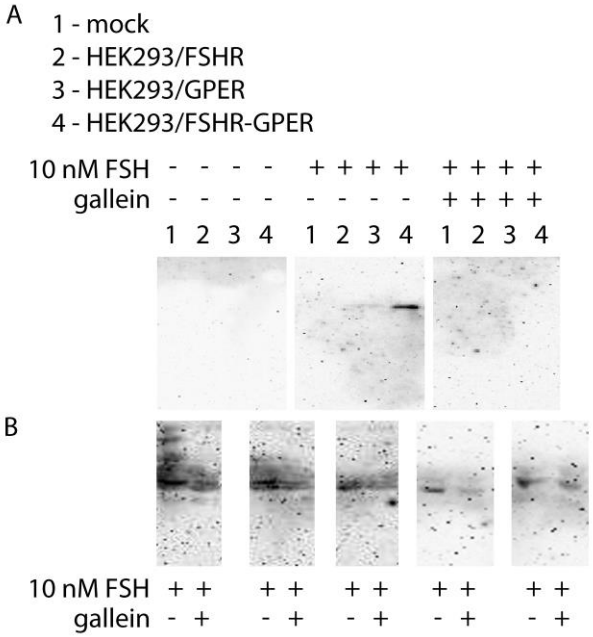

Figure S9. Western blotting analysis of FSH-induced pAKT activation. (**A**) Uncropped Western blotting pAKT membranes of Fig. 4H. (**B**) Experimental replicates of pAKT activation in HEK293/FSHR-GPER cells treated by FSH, in the presence or in the absence of gallein. Signals were acquired by the QuantityOne analysis software (Bio-Rad Laboratories Inc.) and plotted on a box and whiskers graph (Fig. 4I) after background subtraction. Related to Figure 3H.

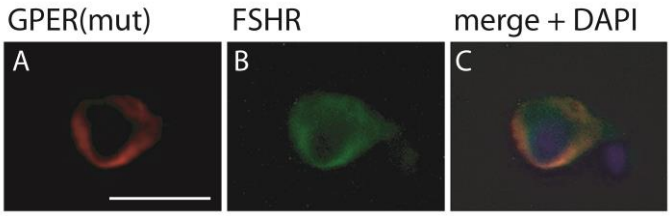

Figure S10. Representative evaluation of GPER(mut) and FSHR co-localization by immunofluorescence, in transfected HEK293 cells. GPER(mut) was detected by the anti-GPER specific primary antibody and TRITC-labelled secondary antibody, while FSHR is identified by the venus tag light emission. Nuclei were blue-stained by DAPI (bar=25 μm). Related to Figure 4G.

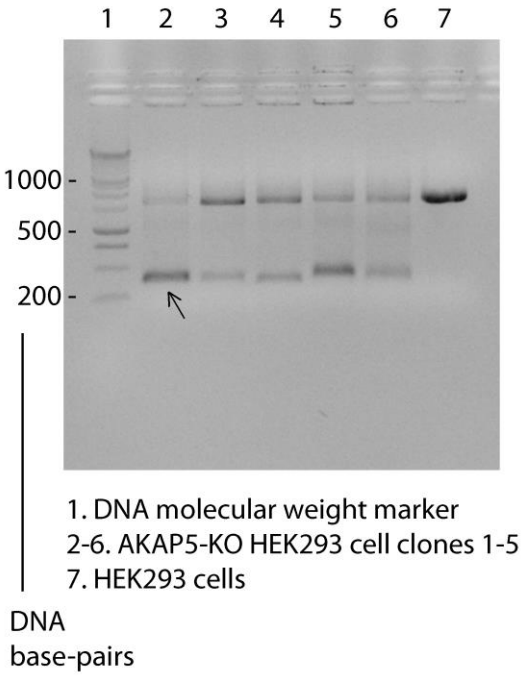

Figure S11. Screening of *AKAP5*-KO HEK293 cells by PCR and 1% agarose-gel electrophoresis. *AKAP5* forward (fwd) and reverse (rev) primers (*GGAGTAAGATGAAAGGTATGAATATGCC* and *CTGCAATCTGTGCTGACTTCC*, respectively; 58°C melting temperature) were designed using the human gene sequence as a template (NC_000014.9). PCR reactions were performed using genomic DNAs extracted from five KO clones (lanes 2-6), while DNA from “native” HEK293 cells was used as a control (lane 7). The predicted sequenced amplified in *AKAP5*-KO cells is of 335 base-pairs, while a band of about 900 base-pairs is predicted to be amplified in the WT *AKAP5*-positive sample. A variable grade of *AKAP5*-WT cell contamination persists among the cultured *AKAP5*-KO HEK293 cells maintained under selective pressure by 1.2 µg/ml puromycin. Arrow indicates the clone used for experiments (Fig. 5). Related to Figure 5A.

Figure S12. *AKAP5* gene and CRISPR/Cas9 targeting. The entire coding region in exon 2 was erased. Sequence of the Cas9 backbone carried in pSpCas9(BB)-2A-Puro (PX459) V2.0 vectors are below and gRNA sequences indicated in bold. Related to Figure 5A.

5’-
AMMTCGMMAWWACGATACAAGCTGTTAGAGAGATAATTGGAATTAATTTGACTGT
AAACACAAAGATATTASTACAAAATACGTGACGTAGAAAGTAATAATTTCTTGGGTA
GTTTGCAGTTTTAAAATTATGTTTTAAAATGGACTATCATATGCTTACCGTAACTTGA
AAGTATTTCGATTTCTTGGCTTTATATATCTTGTGGAAAGGACGAAA**CACCGATCAG**
CAGAAGGTAGTCCTGGTTTTAGAGCTAGAAATAGCAAGTTAAAATAAGGCTAGTCC
GTTATCAACTTGAAAAAGTGGCACCGAGTCGGTGCTTTTTTGTTTTAGAGCTAGAAA
TAGCAAGTTAAAATAAGGCTAGTCCGTTTTTAGCGCGTGCGCCAATTCTGCAGACA
AATGGCTCTAGAGGTACCCGTTACATAACTTACGGTAAATGGCCCGCCTGGCTGA
CCGCCCAACGACCCCCGCCCATTGACGTCAATAGTAACGCCAATAGGGACTTTCC
ATTGACGTCAATGGGTGGAGTATTTACGGTAAACTGCCCACTTGGCAGTACATCAA
GTGTATCATATGCCAAGTACGCCCCCTATTGACGTCAATGACGGTAAATGGCCCGC
CTGGCATTGTGCCCAGTACATGACCTTATGGGACTTTCCTACTTGGCAGTACATCT
ACGTATTAGTCATCGCTATTACCATGGTCGAGGTGAGCCCCACGTTCTGCTTCACT
CTCCCCATCTCCCCCCCCTCCCCACCCCCAATTTTGTATTTATTTATTTTTTAATTAT
TTTGTGCAGCGATGGGGGCGGGGGGGGGGGGGGGGG-3’

5’-
ACMMMCGCMWWAMGATAMAAGGCTGTTAGAGAGATAATTGGAATTAATTTGACT
GTAAACACAAAGATATTAGTACAAAATACGTGACGTAGAAAGTAATAATTTCTTGGG
TAGTTTGCAGTTTTAAAATTATGTTTTAAAATGGACTATCATATGCTTACCGTAACTT
GAAAGTATTTCGATTTCTTGGCTTTATATATCTTGTGGAAAGGACGAAA**CACCGTGA**
CTTACTCTCCAGAGTCAGTTTTAGAGCTAGAAATAGCAAGTTAAAATAAGGCTAGT
CCGTTATCAACTTGAAAAAGTGGCACCGAGTCGGTGCTTTTTTGTTTTAGAGCTAG
AAATAGCAAGTTAAAATAAGGCTAGTCCGTTTTTAGCGCGTGCGCCAATTCTGCAG
ACAAATGGCTCTAGAGGTACCCGTTACATAACTTACGGTAAATGGCCCGCCTGGCT
GACCGCCCAACGACCCCCGCCCATTGACGTCAATAGTAACGCCAATAGGGACTTT

CCATTGACGTCAATGGGTGGAGTATTTACGGTAAACTGCCCACTTGGCAGTACATC
AAGTGTATCATATGCCAAGTACGCCCCCTATTGACGTCAATGACGGTAAATGGCCC
GCCTGGCATTGTGCCCAGTACATGACCTTATGGGACTTTCCTACTTGGCAGTACAT
CTACGTATTAGTCATCGCTATTACCATGGTCGAGGTGAGCCCCACGTTCTGCTTCA
CTCTCCCCATCTCCCCCCCCTCCCCACCCCCAATTTTGTATTTATTTATTTTTTAATT
ATTTTGTGCAGCGATGGGGGCGGGGGGGGGGGGGGGGSC-3’

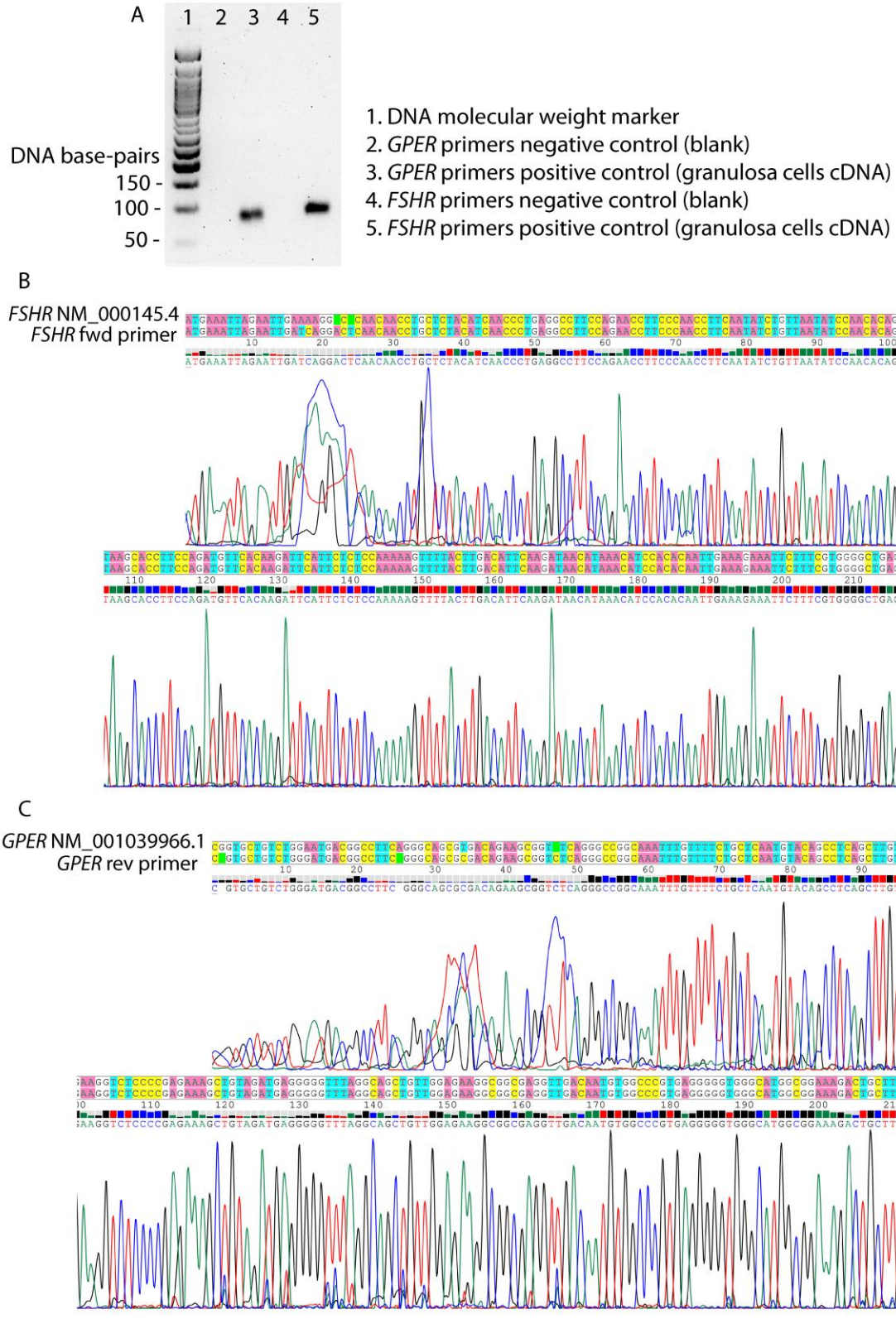
A
1 2 3 4 5
DNA base-pairs
150 -
100 -
50 -
1. DNA molecular weight marker
2. GPER primers negative control (blank)
3. GPER primers positive control (granulosa cells cDNA)
4. FSHR primers negative control (blank)
5. FSHR primers positive control (granulosa cells cDNA)
B
FSHR NM_000145.4
FSHR fwd primer
C
GPER NM_001039966.1
GPER rev primer

Figure S13. Validation of the *FSHR* and *GPER* primer sequences used for real-time PCR analyses. (**A**) Control experiment performed using blank samples and cDNAs from human primary granulosa cells. Analysis by PCR and 1% agarose-gel electrophoresis demonstrates the presence of bands at the predicted molecular weights. (**B**, **C**) Images of partial electropherograms obtained by DNA Sanger's sequencing demonstrating the specificity of the primers used for real-time PCRs displayed in the figure 6 (only one of the two primers per gene is shown). FSHR and GPER BRET plasmids were used as templates. Related to Figure 6D.

Figure S14. Normalizer (*RPS7*) gene expression raw data. Data were obtained from two technical replicates by real-time PCR analysis of normo- and sub-responder women cDNAs. *FSHR* and *GPER* gene expression increase over the *RPS7* level are also indicated. Related to Figure 6D.

Patient ID	**FSHR (fold-increase over *RPS7*)**	**GPER (fold-increase over *RPS7*)**		***RPS7* mean Cq**
		normo-responders	**sub-responders**	
1	0.89	0.87		27.34
3	0.82	0.80		24.51
5	0.89	0.92		28.50
6	0.81	0.79		24.34
7	0.85	0.82		25.32
8	0.84		0.84	25.23
9	0.83		0.85	25.56
10	0.80	0.81		24.99
11	0.81	0.83		24.29
12	0.83	0.82		24.71
13	0.82	0.91		26.92
14	0.81		0.99	31.18
15	0.75		0.88	27.25
16	0.88	0.86		26.89
17	0.85		0.82	25.38
18	0.89	0.86		27.68
19	0.83	0.80		23.77
20	0.72		0.86	23.90
21	0.85	0.87		26.63
22	0.80		0.89	27.18
23	0.78		0.79	23.91
24	0.82	0.81		25.86
25	0.83	0.83		26.32
26	0.87		0.86	26.59
27	0.85	0.84		24.68
28	0.82	0.89		24.37
30	0.86	0.81		26.75
31	0.86		0.84	29.16
32	0.82		0.80	25.83
33	0.84		0.84	28.77
38	0.87	0.87		25.66
40	1.07		0.86	29.79
41	0.76	0.79		25.13
42	0.86	0.91		26.19

45	0.79		0.83	26.13
47	0.92	0.79		26.18
48	0.82	0.75		25.77
52	1.18		0.94	26.40
53	0.98		0.88	25.20
54	0.75	0.76		29.03
55	0.82	0.82		32.44
56	0.71	0.78		28.80
61	0.92	0.82		27.50
63	0.98		0.82	25.86
64	0.70	0.76		28.10
67	0.82		0.82	25.21
70	0.84	0.80		27.21
72	0.82		0.80	28.16
73	0.80	0.80		27.90
74	0.78	0.79		24.57
75	0.88	0.89		26.20
76	0.86	0.87		26.73
77	0.97		0.93	26.88
78	0.94	0.89		27.30
79	0.94	0.90		28.29
82	0.86	0.91		25.68
83	0.79	0.82		28.11
87	0.91	0.93		24.68
88	0.96	0.95		28.59
89	0.89		0.84	28.95
90	1.12	1.12		29.62
91	0.80		0.85	25.04
92	0.73	0.75		26.77
93	0.80	0.77		30.55
94	0.71		0.76	26.00
95	0.83	0.78		26.85
96	0.84		0.78	23.95
97	0.81		0.77	34.32
99	0.86	0.84		31.00
100	0.85		0.81	23.21
101	0.88		0.86	26.09
102	0.87		0.85	24.33
103	0.83		0.80	26.36
104	0.84	0.78		28.42
105	0.91	0.87		23.42
106	1.00	0.99		25.90
107	0.91	0.92		27.19
108	0.83	0.79		29.45
109	0.85	0.77		27.00

110	0.95	0.92		27.26
111	0.86	0.81		30.49
112	0.84	0.83		29.14
113	0.80	0.76		32.76
115	0.78	0.74		30.02
118	0.85	0.77		29.69
119	0.97	0.93		29.17
120	1.03	0.98		25.51
121	NA	NA		25.14
122	1.09	1.01		24.15
123	0.98	0.96		26.37
124	0.93	0.84		25.16
125	0.84		0.77	27.13

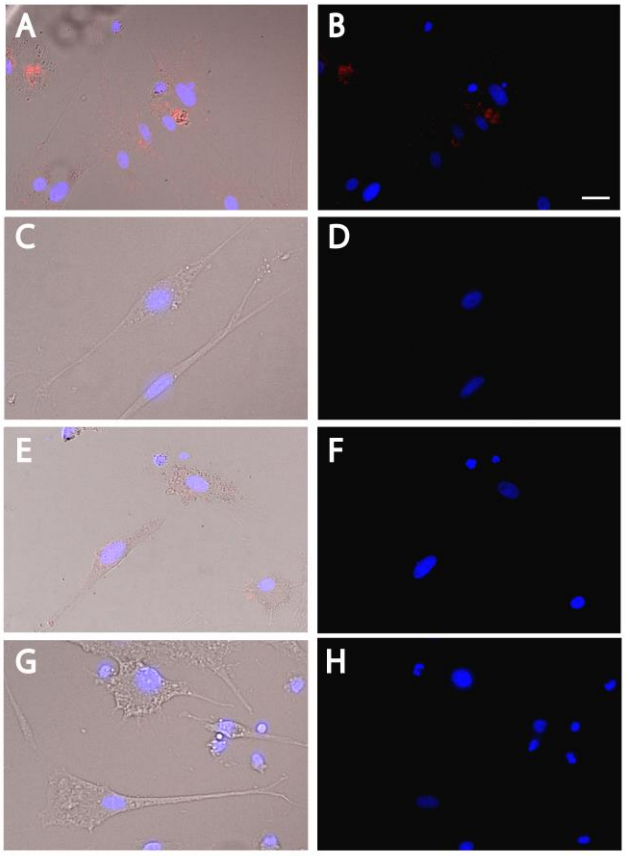

Figure S15. Representative evaluation of FSHR-GPER interaction by proximity ligation assay. Fixed human primary granulosa cells were treated by specific primary antibodies against GPER and FSHR before sample incubation with “PLUS” and “MINUS” probes, and red detection reagents (see Supplementary materials and methods). Nuclei were blue-stained by DAPI and signals captured by a fluorescent microscope (bar=40 μm); images representative of three independent experiments. (**A, B**) Bright field and fluorescence images of positive (red) signals indicating FSHR-GPER interaction. (**C, D**) Negative controls obtained in the absence of the “PLUS” probe. (**E, F**) Negative controls, absence of the “MINUS” probe. (**G, H**) Negative controls prepared without incubation with primary antibodies. Related to Figure 6C, E-J.

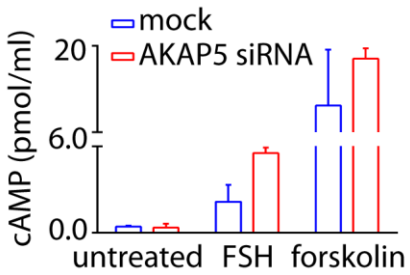

Figure S16. FSH-induced cAMP increase under 48-h AKAP5 knockdown by siRNA. Human primary granulosa cells were treated 30 min with 10 nM FSH, in the presence of IBMX, before cAMP measurement by HTRF. Results are means ± SD of two experiments and forskolin-treated samples served as positive controls. FSH treatment induced 2.6-fold FSH levels in AKAP5-depleted than mock-transfected cells. Related to Figure 6K.

Transparent Methods

Study design.

The objective of this study in vitro was to determine the impact of FSHR-GPER heteromers in modulating FSH impact on cell viability. Experiments were performed in biological triplicate, unless otherwise stated, on the basis of previous experiences using transfected cell lines and primary cells in vitro. Studies with granulosa cells collected from donor poor- and normo-responder women undergoing oocyte retrieval for assisted reproduction techniques were performed with n=30 and 61 samples, which have a power of about 95% to detect a difference of 1.7% between the r2 values of two groups (alpha=0.05). Experiments were blinded to the operator performing cell handling and real-time PCR analyses. Written consent was collected from women under local Ethics Committee permission (Nr. 796 19th June 2014, Reggio Emilia, Italy). Patients matched these criteria: absence of endocrine abnormalities and viral/bacterial infections, age between 25 and 45 years.

Cell lines and reagents.

The HEK293 cell line was available in-house and previously validated for BRET experiments (Lazzaretti et al., 2019; Riccetti et al., 2017a). The culture medium was Dulbecco's Modified Eagles Medium (DMEM) enriched by 10% fetal bovine serum (FBS), 2 mM L-glutammine, 100 U/ml penicillin and 50 µg/ml streptomycin.

Human primary granulosa cells were collected from ovarian follicles of donor women classified as poor- (≤4 oocytes collected after controlled ovarian stimulation) or normo-responders (>4 oocytes), as indicated by a previous consensus paper (Ferraretti et al., 2011) and more recent evidences suggesting that ovarian response may be categorized as poor, suboptimal, normal and high (Polyzos and Sunkara, 2015). Women were clinically treated in a GnRH antagonist protocol, where ovarian stimulation was performed by FSH and oocyte trigger with hCG. Normo- and sub-responder groups differ for the number of oocytes (8.1 ± 3.2 *vs* 2.6 ± 1.2, respectively), serum E_2 levels at the day of oocytes collection (1895.0 ± 866.9 *vs* 1348.0 ± 838.2 pg/ml) and total FSH

dose for achieving the oocyte maturation (2895.0 ± 4378.0 *vs* 3642.0 ± 3010.0 IU; Mann-Whitney's U-test, $p<0.05$), while the duration of the stimulation cycle was similar between the two groups (12.6 ± 3.2 *vs* 13.7 ± 3.5 days; Mann-Whitney's U-test, $p\geq0.05$). Granulosa cells were handled as previously described (Riccetti et al., 2019) and cultured in McCoy's 5A medium, 10% FBS, 2 mM L-glutamine, 100 IU/ml penicillin, 100µg/ml streptomycin and 250 ng/ml Fungizone. All culture reagents were from Sigma-Aldrich (Sigma-Aldrich Corporation, St. Louis, MO, USA).

Recombinant FSH was provided by Merck KGaA (Gonal-f; Merck KGaA, Darmstadt, Germany) and used at the concentration of 10 nM as previously described (Lazzaretti et al., 2019), while E_2 (cat. E8875; 50 pg/ml) (Casarini et al., 2017), 8-br-cAMP (B7880; $1x10^{-15}$-10^{0} nM range) (Lazzaretti et al., 2019), forskolin (F6886; 50 µM) (Casarini et al., 2016), gallein (cat. 371708; 10 µM) (Sanz et al., 2017), fulvestrant (I4409; 2 µg/ml) (Wakeling et al., 1991) and triton-X (T8787; 5%) were purchased by Sigma-Aldrich. Three human GPER siRNA probes (284631; 3x10 µM/probe) were purchased by ThermoFisher Scientific (Waltham, MA, USA) and delivered into cells using the TransIT TKO transfection reagent (Mirus Bio Corporation, Madison, WI, USA). The AKAP5-encoding gene was silenced by using the TriFECTa® RNAi kit (#hs.Ri.AKAP5.13; Integrated DNA Technologies, Coralville, IA, USA). The control siRNA was the #4390843 Silencer™ Negative Control No. 1 siRNA (Thermo Fisher Scientific).

FSHR-, LHCGR-, Ca^{2+} aequorin- and cAMP CAMYEL-encoding BRET biosensor and cFMS plasmids were available in-house and previously validated (Lazzaretti et al., 2019; Riccetti et al., 2017a, 2019; Sposini et al., 2015). GPER- and GPER(mut)-encoding BRET biosensor plasmids were developed by *de novo* synthesis and checked by the producer (Gene Universal Inc., Newark, DE, USA), basing on the FLAG/GPER-encoding plasmid (Albanito et al., 2008) provided by professor Marcello Maggiolini (University of Calabria, Cosenza, Italy). Gα protein-encoding BRET biosensor plasmids (Wan et al., 2018) were kindly provided by professor Nevin A. Lambert (Augusta University, Augusta, GA, USA). Cell transfections using plasmids were performed using Metafectene PRO (Biontex Laboratories GmbH, Munich, Germany).

BRET and HTRF measurements, and ELISA.

Intracellular Ca^{2+} and cAMP levels were evaluated following a validated procedure (Brigante et al., 2019; Casarini et al., 2019; Lazzaretti et al., 2019; Riccetti et al., 2017b, 2017a, 2019), in transiently transfected HEK293 cells. G protein coupling experiments were adapted to optimize BRET signals with GPER- and FSHR-encoding plasmids (100 ng plasmid/well as reference amount), starting from the published validation protocol (Wan et al., 2018). BRET signals were induced using 10 µl/well of 5µM Coelenterazine h (Interchim, Montluçon, France) diluted in 40 µl/well PBS and 1 mM Hepes, in the presence or in the absence of hormones/vehicle. Light emissions were detected at 475±30 and 530±30 nm wavelengths by the CLARIOstar plate reader equipped with a monochromator (BMG Labtech, Ortenberg, Germany). Assessment of protein content was used as loading controls for BRET experiment, while linearity between amount of plasmid administered per well and receptor expressed was confirmed detecting signals of the biosensor-tag.

In granulosa cells and in the GPER(mut)-expressing cell line, cAMP production was measured using an ELISA kit (ab65355; Abcam, Cambridge, UK) following the manufacturer's instructions and signals acquired by a Victor3 plate reader (Perkin Elmer Inc., Waltham, MA, USA). Alternatively, cAMP was measured in granulosa cells by homogeneous time-resolved fluorescence (HTRF) where indicated. The assay was performed using the cAMP dynamic 2 assay kit and following the provider's instructions (CisBio Bioassays, Bagnol sur Cèze, France). Cells were treated with ligands three h in the presence of 50 µM of the phosphodiesterase inhibitor 3-isobutyl-1-methylxanthine (IBMX; Sigma-Aldrich) before to be lysed and transferred into white 384-well microplates. 10 µl/well of the supplied conjugate-lysis buffer, containing d2-labeled cAMP and Europium cryptate-labeled anti-cAMP antibody, was added. Plates were incubated for 1 h in the dark at room temperature and signals measured at 620 and 665 nm, 50 ms after excitation at 320 nm using the CLARIOstar plate reader (BGM Labtec).

Viability assay.

The 3-(4,5-dimethylthiazol-2-yl)-2,5-diphenyltetrazolium bromide (MTT) assay was performed according the manufacturer's instruction and previous optimizations (Casarini et al., 2016, 2017). The assay solution was prepared starting from the powder commercially available (M5655; Sigma-Aldrich) and left into cell well-plates 4 h before to be lysed with isopropanol and determine absorbance value by a plate reader.

PD-PALM imaging and localization analysis.

PD-PALM imaging was carried out as previously described (Jonas et al., 2015). Briefly, anti-FLAG and anti-HA antibodies were labelled with CAGE 500 and 552 photoswitchable dyes, respectively, following manufacturer's protocol (Abberior GmbH, Göttingen, Germany). Degree of labelling was determined to be 1.0 ± 0.2 dye molecules per antibody and 1.3 ± 0.1 dye molecules per antibody for FLAG-CAGE 500 and HA-CAGE 552 respectively. HEK293 cells were transfected with 0.5 µg FLAG-tagged GPER or GPER(mut), and 1 µg HA-tagged FSHR per well of a 6-well plate. Transfected cells were seeded onto 1.5 glass bottom dishes (MatTek Corporation, Ashland, MA, USA). Cells were incubated with CAGE-conjugated antibodies at 37 °C for 30 min. Cells were washed with PBS and fixed in 4% paraformaldehyde with 0.2% glutaraldehyde for 30 min. Cells were washed with DPBS and maintained in DPBS in the dark until imaging. Simultaneous dual-color images were acquired using an Elyra PS1 (Carl Zeiss AG, Oberkochen, Germany). Images were obtained at 100x oil emersion, 1.45 NA objective. Photo-conversion of CAGE 500 and 552 dyes was achieved with 405 nm light source and was simultaneously imaged and photo-bleached by 491 and 561 nm lasers, respectively. Acquisition of images is as previously described (Jonas et al., 2015).

Analysis was carried out on cropped non-overlapping 2 × 2 µm regions, within cell-cell boundaries, from 491- and 561-nm channels and analyzed for localized receptors by QuickPALM Fiji plugin to generate x-y coordinates of localized receptors in each channel. The number of associated protomers derived from the *x-y* coordinates were quantified using a custom Java application (PD-Interpreter) (Jonas et al., 2015). The percentage and protomer composition of FSHR, GPER and GPER(mut) homomers and heteromers was carried out using a second order Getis Franklin neighbourhood analysis with a search radius of 50 nm. This radius has been previously employed for

gonadotrophin hormone receptors based on localization precision, the large extracellular domain of FSHR and the maximum distance that labelling of the antibody would concur, ~15-20 nm (Roberts et al., 1995). Outputted data was represented as a co-localization plot with heat maps generated to represent the different numbers of associated protomers observed.

Protein analysis.

Protein content of samples was determined by the colorimetric Bradford assay using a commercial reagent and following the manufacturer's instructions (#5000201; Bio-Rad Laboratories Inc., Hercules, CA, USA), then 595-nm signals were acquired by a plate reader. Target proteins were analyzed by 12% SDS-PAGE and Western blotting using a validated protocol (Bates et al., 2006; Casarini et al., 2012, 2016, 2017) after extraction in ice-cold RIPA buffer along with PhosStop phosphatase inhibitor and a protease inhibitor cocktail (Roche, Basel, Switzerland). Human pAKT, -pCREB and total ERK (#9271, #9198, #4695, respectively; Cell Signaling Technology Inc., Danvers, MA, USA), active/pro caspase 3 (#MA1-91637; Thermo Fisher Scientific, MA, USA), FSHR (#PA5-28764; ThermoFisher Scientific, Waltham) and GPER (#AF5534; Bio-Techne Corporation, Minneapolis, MN, USA) were evaluated using specific antibodies and secondary anti-rabbit (#NA9340V; GE HealthCare) or -goat HRP-conjugated antibodies (#ab6885; Abcam), as appropriate. A mouse HRP-conjugated anti-human β-ACTIN antibody (#A3854; Sigma-Aldrich) was also used. Signals were developed with ECL (GE HealthCare), detected and semi-quantified by VersaDoc system using the QuantityOne analysis software (Bio-Rad Laboratories Inc.).

Steroid hormone measurements.

Serum FSH levels were calculated as the cumulative dose injected in patients throughout the ovarian stimulation period. Total progesterone and estradiol was measured in sera and in the cell media (4×10^4 cells/well), as indicated, by an immunoassay analyzer (ARCHITECT second Generation system; Abbot Diagnostics, Chicago, IL, USA) after freezing-thawing samples (Riccetti et al., 2019) and data normalized over cell amount.

Structural modeling.

No crystallographic structures are available so far for GPER. Structural models of the two receptors (human species) deprived of the N-terminal and C-terminal regions were achieved by comparative modeling (by the Modeler software (Sali and Blundell, 1993)) by using the crystal structure of an inactive state of the μ-opioid receptor (PDB: 4dkl) as a template, according to a protocol already described (Fanelli and De Benedetti, 2011). As for the FSHR, to model the insertions, the following portions: 488-490 (in E1), 580-583 (in E2), 617-621 and 628-631 (both in I3), and 669-671 (in E3) were deleted in the template crystal structure, followed by addition of external α-helical restraints to the following amino acid stretches: 421-432 (extracellular extension of H2), and 552-559 (cytosolic extension of H6). As for GPER to model the insertions, the following portions: 219-230 (C-terminal portion of E2 and initial portion of H5), 222-225 (in E2), 259-263 and 270-273 (both in I3), and 307-311 (in E3) were deleted in the template crystal structure, followed by addition of external α-helical restraints to the following amino acid stretches: 52-62 (cytosolic half of H1), 226-233 (cytosolic extension of H5), 241-244 (cytosolic extension of H6), 271-278 (extracellular extension of H6), and 286-293 (extracellular extension of H7). For each receptor, one-hundred models were built by randomizing all the Cartesian coordinates of standard residues in the initial model. The best model according to quality checks was subjected to application of rotamer libraries to those side chains in non-allowed conformation.

Prediction of likely architectures of FSHR-GPER heterodimer followed a computational approach developed for quaternary structure predictions of transmembrane α-helical proteins, defined as a FiPD-based approach (Casciari et al., 2006; Fanelli et al., 2013). It consists in rigid-body docking using a version of the ZDOCK program devoid of desolvation as a component of the docking score (v2.1) (Chen et al., 2003). FSHR was used as a fixed protein (target) and GPER as a mobile protein (probe) and vice versa in two distinct docking runs. A rotational sampling interval of 6º was set (i.e., dense sampling) and the best 4000 solutions were retained and ranked according to the ZDOCK score. Such solutions were filtered according to the “membrane topology” filter (by using the FiPD software (Casciari et al., 2006), which discards all those solutions that violate the membrane topology requirements. The membrane topology filter, indeed, discards all the solutions characterized by a deviation

angle from the original z-axis, i.e. tilt angle, and a displacement of the geometrical centre along the z-axis, i.e. z-offset, above defined threshold values, which were 0.4 radians and 6.0 Å, respectively. The filtered solutions from each run were merged with the target protein, leading to an equivalent number of dimers that were clustered using a C_α-RMSD threshold of 3.0 Å for each pair of superimposed dimers. All the amino acid residues in the dimer were included in C_α-RMSD calculations. Cluster analysis was based on a QT-like clustering algorithm (Heyer et al., 1999) implemented both in the FiPD and Wordom software (Casciari et al., 2006; Seeber et al., 2011). Since the filtering cutoffs of the membrane topology parameters are intentionally quite permissive, inspection of the cluster centres (i.e. the solutions with the highest number of neighbours in each cluster) served as a final filter to discard remaining false positives, thereby leading to a dramatic reduction of the reliable solutions. The best scored docking solutions from the most populated and reliable clusters were finally considered. Cluster reliability was based on the MemTop score, accounting for the goodness of the membrane topology. Such index is defined according to the following formula:

$$MemTop = \sqrt{\left\langle tilt_{nor} \right\rangle^2 + \left\langle Z_{offnor} \right\rangle^2}$$

where, the squared terms are, respectively, the normalized tilt angle and the z-offset averaged over all the members of a given cluster. Normalization of each tilt angle and z-offset value was carried out by dividing each value for the respective cutoff value, i.e. 0.4 radians, for the tilt angle, and 6.0 Å, for the z-offset. The optimal value for such index is zero.

Final selection of the likely heterodimer relied on a consensus from the two different docking runs.

CRISPR/Cas9 experiments.

Since AKAP5 is encoded by a single exon (exon 2), two guide RNA probes (gRNAs) were used to excise the entire genetic region (PubMed Gene ID: 9495; last update: 1 June 2020). gRNAs were designed using Benchling platform and then ordered as a synthetic DNA fragment (Gene Strings, Thermo Fisher Scientific) flanked

by two restriction enzyme BbsI recognition sites. Each of the two double-stranded DNA fragment was then cloned into a pSpCas9(BB)-2A-Puro (PX459) V2.0 vector, respectively, which was a gift from Feng Zhang (#62988; Addgene, Watertown, MA, USA), using digestion/ligation protocol (Ran et al., 2013). The vectors were then amplified and purified from ampicillin-resistant bacteria with Zyppy Mini Plasmid Kit (Zymo Research, Irvine, CA, USA).

HEK293 cells transfection was performed using TurboFect reagent (Thermo Fisher Scientific) according to manufacturer protocol. After 48 h, we enriched cell media by 1.2 µg/ml puromycin before to verify the KO by PCR reaction in single clone lysates.

Immunofluorescence and immunohistochemistry.

FSHR and GPER expression was detected by immunofluorescent microscopy in both granulosa and 48-h transfected HEK293 cells using a ZOE Fluorescent Cell Imager (Bio-Rad Laboratories Inc.). Granulosa cells were fixed by 3-min treatment with 4% ice-cold paraformaldehyde/PBS, heated 20 s x 600 W in a microwave and incubated with 20 µg/ml rabbit anti-FSHR (#PA5-28764; ThermoFisher Scientific) and/or 20 µg/ml goat anti-GPER (#LS-B5132; LifeSpan BioSciences, Inc., Seattle, WA, USA) primary antibodies. Secondary antibodies were donkey anti-rabbit FITC and anti-goat TRITC (#ab6798 and #ab6882; Abcam). In transfected HEK293 cells, treatment by the anti-GPER and proper secondary antibody was performed, while FSHR was identified by the venus-tag emission. 300 nM DAPI was used for staining nuclei.

Immunohistochemistry was performed using an R.T.U. Vectastain Universal Elite ABC kit and DBA Substrate Kit (both from Vector Laboratories, Burlingame, CA, USA) according to the manufacturer's instructions. Briefly, paraffin-embedded ovarian tissues of fertile women at the follicular stage, stored in a pathological anatomy laboratory, were sliced into 5 µm sections, deparaffinized and hydrated using decreasing concentration of ethanol. Antigen retrieval was performed by heating sections for 10 min in sodium citrate buffer (pH = 6.0), followed by cooling at room temperature. After treatment for 10 min with 3% hydrogen peroxide in deionized water to quench endogenous peroxidases and for 30 min with normal horse serum (NHS) (Vector Laboratories, Burlingame, CA), sections were incubated overnight at 4°C with primary antibodies diluted in 0.3% NHS in

PBS: 20 µg/ml rabbit anti-FSHR (#PA5-28764; ThermoFisher Scientific, Waltham, MA, USA) or 20 µg/ml rabbit anti-GPER (#LS-A4271; LifeSpan BioSciences Inc., Seattle, WA, USA). Control sections were incubated with 0.3% NHS in PBS in the absence of primary antibody. Slides were incubated in biotinylated horse anti-rabbit (Vector Laboratories, Burlingame, CA) for 30 min at RT followed by 30 min in Elite ABC reagent (Vector Laboratories, Burlingame, CA). Visualization of antibody binding was achieved applying DAB solution (Vector Laboratories, Burlingame, CA) for 5 min. Sections were then counterstained with hematoxylin, dehydrated and mounted using a non-aqueous mounting medium. Images were acquired by Zeiss Axioplan 2 microscope equipped with a Nikon Digital Sight camera.

Proximity ligation assay.

FSHR and GPER interaction was confirmed by proximity ligation assay (PLA) in human primary granulosa cells. Samples were seeded on glass slides and fixed by 4% ice-cold paraformaldehyde/PBS before to be incubated with 20 µg/ml rabbit anti-FSHR (#PA5-28764; ThermoFisher Scientific) and/or 20 µg/ml goat anti-GPER (#LS-B5132; LifeSpan BioSciences, Inc.) primary antibodies. Cells were washed twice with PBS after each protocol step. PLA was applied using the Duolink® In Situ Red Starter Goat/Rabbit kit and following the supplier instructions (#DUO92105-1KT; Sigma-Aldrich). Briefly, samples were incubated 1 h with anti-goat and -rabbit secondary antibodies bound to short DNA strands. These compounds are called “PLUS” and “MINUS” PLA probes and their DNA strands can interact through a subsequent addition of two other circle-forming DNA oligonucleotides whether they are in close proximity (<40 nm). The two oligonucleotides were joined by enzymatic ligation and amplified using a polymerase, forming a rolling circle DNA. Several-hundredfold replications of the DNA circle occur and labeled complementary oligonucleotide probes highlight the product. Therefore, the resulting high concentration light emission may be visible with a fluorescence microscope and indicates the interaction between the two targets. Negative controls were prepared by incubation of samples without the “PLUS”, the “MINUS” probe or the primary antibodies. Slides were then closed using a mounting medium containing DAPI and provided in the PLA kit. Images were acquired using the ZOE Fluorescent Cell Imager (Bio-Rad Laboratories Inc.).

Gene expression and DNA sequencing analysis.

Gene expressions were evaluated using specific primer sequences. *FSHR* (NM_000145.3): fwd 5′-GGAGGTGATAGAGGCAGATG-3′; rev 5′-GGGTTGATGTAGAGCAGGT- 3′; *GPER* (AF027956): fwd 5'-CTGAACCGCTTCTGTCAC-3'; rev 5'-ACTGCTGAACCTCACATC-3'. The *RPS7* housekeeping gene was the loading control (NM_001011.4; fwd: 5'-AATCTTTGTTCCCGTTCCTCA-3'; rev 5'-CGAGTTGGCTTAGGCAGAA-3'). Primers were validated by PCR and DNA Sanger sequencing (Figure S2), performed using known settings (Lazzaretti et al., 2019).

Flow Cytometry.

HEK293 cells were transiently transfected with either plasmid encoding for empty pcDNA3.1 vector (mock) or increasing concentrations of FLAG-tagged FSHR- or untagged GPER-encoding plasmids. To evaluate the relative expression and localization of FSHR and GPER proteins in the cell membrane, cells were also co-transfected with a fixed concentration of FLAG-tagged FSHR- and increasing concentrations of GPER-encoding plasmids. Cells were detached, washed and resuspended in working buffer (PBS without Ca^{2+} and Mg^{2+}; 1% BSA, 2 mM EDTA) 48 hours after transfection. Then, cells were incubated with phycoerythrin (PE)-conjugated anti-FLAG antibody (anti-DYKDDDDK-PE, #130-101-577; 1:100 dilution; Milteny Biotech, Bergisch Gladbach, Germany), 1 h at 4°C, to reveal membrane expression of FSHR. GPER cell membrane expression was revealed by incubating transfected cells 2 h at 4°C with anti-GPER primary antibody (#LS-A4271; LifeSpan BioSciences Inc.) followed by incubation with secondary antibody Alexa Fluor 647-conjugated AffiniPure (1:100 dilution; #AS075 Jackson Laboratory, Bar Harbor, USA), 1 h at 4°C. Cells were washed twice and re-suspended in working buffer before analysis with MACSQuant Analyzer 10 Flow cytometer (Milteny Biotech). Data were analysed and plotted with the FlowJo software (FlowJo, Ashland, OR, USA).

Statistical analysis.

The D'Agostino and Pearson normality test was performed before choosing to use parametric or non-parametric statistics. Two groups of samples were compared

using Mann-Whitney's U-test or t-test, while multiple groups were compared using Kruskal-Wallis or one-/two-way ANOVA as proper, as well as proper post-tests and corrections for multiple comparisons depending on the nature of data. Groups were represented in column graph using box and whiskers plots. Non-linear and linear regressions were used for data interpolation in x-y graphs and two linear regressions were compared using the parallelism test of slopes. Statistics were performed using the GraphPad Prism 6.0 software (GraphPad Software Inc., La Jolla, CA, USA).

Supplementary references

Albanito, L., Sisci, D., Aquila, S., Brunelli, E., Vivacqua, A., Madeo, A., Lappano, R., Pandey, D.P., Picard, D., Mauro, L., et al. (2008). Epidermal Growth Factor Induces G Protein-Coupled Receptor 30 Expression in Estrogen Receptor-Negative Breast Cancer Cells. Endocrinology *149*, 3799–3808.

Bates, B., Zhang, L., Nawoschik, S., Kodangattil, S., Tseng, E., Kopsco, D., Kramer, A., Shan, Q., Taylor, N., Johnson, J., et al. (2006). Characterization of Gpr101 expression and G-protein coupling selectivity. Brain Res. *1087*, 1–14.

Brigante, G., Riccetti, L., Lazzaretti, C., Rofrano, L., Sperduti, S., Potì, F., Diazzi, C., Prodam, F., Guaraldi, G., Lania, A.G., et al. (2019). Abacavir, nevirapine, and ritonavir modulate intracellular calcium levels without affecting GHRH-mediated growth hormone secretion in somatotropic cells in vitro. Mol. Cell. Endocrinol. *482*, 37–44.

Casarini, L., Lispi, M., Longobardi, S., Milosa, F., La Marca, A., Tagliasacchi, D., Pignatti, E., and Simoni, M. (2012). LH and hCG Action on the Same Receptor Results in Quantitatively and Qualitatively Different Intracellular Signalling. PLoS One *7*, e46682.

Casarini, L., Reiter, E., and Simoni, M. (2016). β-arrestins regulate gonadotropin receptor-mediated cell proliferation and apoptosis by controlling different FSHR or LHCGR intracellular signaling in the hGL5 cell line. Mol. Cell. Endocrinol. *437*, 11–21.

Casarini, L., Riccetti, L., De Pascali, F., Gilioli, L., Marino, M., Vecchi, E., Morini, D., Nicoli, A., La Sala, G.B., and Simoni, M. (2017). Estrogen Modulates Specific Life and Death Signals Induced by LH and hCG in Human Primary Granulosa Cells In Vitro. Int. J. Mol. Sci. *18*, 926.

Casarini, L., Riccetti, L., Limoncella, S., Lazzaretti, C., Barbagallo, F., Pacifico, S., Guerrini, R., Tagliavini, S., Trenti, T., Simoni, M., et al. (2019). Probing the Effect of Sildenafil on Progesterone and Testosterone Production by an Intracellular FRET/BRET Combined Approach. Biochemistry *58*, 799–808.

Casciari, D., Seeber, M., and Fanelli, F. (2006). Quaternary structure predictions of transmembrane proteins starting from the monomer: a docking-based approach. BMC

Bioinformatics *7*, 340.

Chen, R., Li, L., and Weng, Z. (2003). ZDOCK: An initial-stage protein-docking algorithm. Proteins Struct. Funct. Genet. *52*, 80–87.

Cheng, S.-B., Dong, J., Pang, Y., LaRocca, J., Hixon, M., Thomas, P., and Filardo, E.J. (2014). Anatomical location and redistribution of G protein-coupled estrogen receptor-1 during the estrus cycle in mouse kidney and specific binding to estrogens but not aldosterone. Mol. Cell. Endocrinol. *382*, 950–959.

Fanelli, F., and De Benedetti, P.G. (2011). Update 1 of: computational modeling approaches to structure-function analysis of G protein-coupled receptors. Chem. Rev. *111*, PR438-535.

Fanelli, F., Seeber, M., Felline, A., Casciari, D., and Raimondi, F. (2013). Quaternary structure predictions and structural communication features of GPCR dimers. Prog. Mol. Biol. Transl. Sci. *117*, 105–142.

Ferraretti, A.P., La Marca, A., Fauser, B.C.J.M., Tarlatzis, B., Nargund, G., Gianaroli, L., and ESHRE working group on Poor Ovarian Response Definition (2011). ESHRE consensus on the definition of “poor response” to ovarian stimulation for in vitro fertilization: the Bologna criteria. Hum. Reprod. *26*, 1616–1624.

Heyer, L.J., Kruglyak, S., and Yooseph, S. (1999). Exploring expression data: identification and analysis of coexpressed genes. Genome Res. *9*, 1106–1115.

Jonas, K.C., Fanelli, F., Huhtaniemi, I.T., and Hanyaloglu, A.C. (2015). Single Molecule Analysis of Functionally Asymmetric G Protein-coupled Receptor (GPCR) Oligomers Reveals Diverse Spatial and Structural Assemblies. J. Biol. Chem. *290*, 3875–3892.

Lazzaretti, C., Riccetti, L., Sperduti, S., Anzivino, C., Brigante, G., De Pascali, F., Potì, F., Rovei, V., Restagno, G., Mari, C., et al. (2019). Inferring biallelism of two FSH receptor mutations associated with spontaneous ovarian hyperstimulation syndrome by evaluating FSH, LH and HCG cross-activity. Reprod. Biomed. Online *38*, 816–824.

Polyzos, N.P., and Sunkara, S.K. (2015). Sub-optimal responders following controlled ovarian stimulation: an overlooked group? Hum. Reprod. *30*, 2005–2008.

Ran, F.A., Hsu, P.D., Wright, J., Agarwala, V., Scott, D.A., and Zhang, F. (2013). Genome engineering using the CRISPR-Cas9 system. Nat. Protoc. *8*, 2281–2308.

Riccetti, L., Yvinec, R., Klett, D., Gallay, N., Combarnous, Y., Reiter, E., Simoni, M., Casarini, L., and Ayoub, M.A. (2017a). Human Luteinizing Hormone and Chorionic Gonadotropin Display Biased Agonism at the LH and LH/CG Receptors. Sci. Rep. *7*, 940.

Riccetti, L., Klett, D., Ayoub, M.A., Boulo, T., Pignatti, E., Tagliavini, S., Varani, M., Trenti, T., Nicoli, A., Capodanno, F., et al. (2017b). Heterogeneous hCG and hMG commercial preparations result in different intracellular signalling but induce a similar long-term progesterone response in vitro. MHR Basic Sci. Reprod. Med. *23*, 685–697.

Riccetti, L., Sperduti, S., Lazzaretti, C., Klett, D., De Pascali, F., Paradiso, E., Limoncella, S., Potì, F., Tagliavini, S., Trenti, T., et al. (2019). Glycosylation Pattern and in vitro Bioactivity of Reference Follitropin alfa and Biosimilars. Front. Endocrinol. (Lausanne). *10*, 503.

Roberts, C.J., Williams, P.M., Davies, J., Dawkes, A.C., Sefton, J., Edwards, J.C., Haymes, A.G., Bestwick, C., Davies, M.C., and Tendler, S.J.B. (1995). Real-Space Differentiation of IgG and IgM Antibodies Deposited on Microtiter Wells by Scanning Force Microscopy. Langmuir *11*, 1822–1826.

Sali, A., and Blundell, T.L. (1993). Comparative protein modelling by satisfaction of spatial restraints. J. Mol. Biol. *234*, 779–815.

Sanz, G., Leray, I., Muscat, A., Acquistapace, A., Cui, T., Rivière, J., Vincent-Naulleau, S., Giandomenico, V., and Mir, L.M. (2017). Gallein, a Gβγ subunit signalling inhibitor, inhibits metastatic spread of tumour cells expressing OR51E2 and exposed to its odorant ligand. BMC Res. Notes *10*, 541.

Seeber, M., Felline, A., Raimondi, F., Muff, S., Friedman, R., Rao, F., Caflisch, A., and Fanelli, F. (2011). Wordom: a user-friendly program for the analysis of molecular structures, trajectories, and free energy surfaces. J. Comput. Chem. *32*, 1183–1194.

Sposini, S., Caltabiano, G., Hanyaloglu, A.C., and Miele, R. (2015). Identification of transmembrane domains that regulate spatial arrangements and activity of prokineticin

receptor 2 dimers. Mol. Cell. Endocrinol. *399*, 362–372.

Wakeling, A.E., Dukes, M., and Bowler, J. (1991). A potent specific pure antiestrogen with clinical potential. Cancer Res. *51*, 3867–3873.

Wan, Q., Okashah, N., Inoue, A., Nehmé, R., Carpenter, B., Tate, C.G., and Lambert, N.A. (2018). Mini G protein probes for active G protein–coupled receptors (GPCRs) in live cells. J. Biol. Chem. *293*, 7466–7473.